17th Brazilian Congress of Thermal Sciences and Engineering
November 25th-28th, 2018, Águas de Lindóia, SP, Brazil

ENCIT-2018-0728

A COMPARISON BETWEEN TWO DIFFERENT CONFIGURATION RADIANT POROUS BURNER FOR PREMIXED COMBUSTION

João Fabrício Manoel
Thiago Augusto Michels
Roberto Wolf Francisco Junior
State University of Santa Catarina. Mechanical Engineering Department, Joinville, Santa Catarina, Brazil.
joaofabriciom@gmail.com

Abstract. *This work aims to analyze the performance of two different configuration porous burner made of silicon carbide operating with premixed combustion of LPG (liquefied petroleum gas). One of the configurations has a decrease of porous media downstream area. The other configuration remains the same, but both have two-layer porous media with different porosities and pore length. The main parameters discussed are the flame stability, the temperature profile in the porous medium and the radiation efficiency for the same equivalence ratio. This study indicated that the temperature profile and flame stability had the same behavior but the temperature on the surface had a difference for an operating range. The radiation efficiency decayed for the burner with smaller downstream area and bigger length, since thermal radiation is directly proportional to area.*

Keywords: *Flame stability, Premixed combustion, Radiant porous burner, Radiation efficiency*

1. INTRODUCTION

With the decrease of fossil fuels reserves over the decades, climate change and energy concern have led to more interest in the study of combustion and enhancement of thermal systems. Thus, there is a need to maximize the recoverable heat and improve the efficiency of combustion systems. In this context, comes the porous burner. It has attracted attention over the past decades and came as a technology to improve the combustion inside burners. Porous burners are made of a metallic or ceramic porous structure where the combustion reaction occurs. The concept of this configuration is to utilize the product energy in the post combustion region to preheat the incoming mixture of the large amount of available enthalpy in the exhaust gas stream (Wood & Harris, 2008).

According to Pereira (2002), porous burners are characterized by high rates of thermal radiation that comes from the solid medium, high combustion efficiency and low emission of pollutants. The main advantages of the porous burners are the wide range of operation limits, low pollutant emissions and high radiation efficiency (Li and Hsu, 2006). It is also important to note that, unlike a conventional free flame, porous burners have a range of speeds where a stable flame can be obtained.

The most commonly materials of porous burner are the reticulated foams. They have advantages such as improved gas mixing, reduced weight and low pressure loss (Gao, et al., 2014b). Most of ceramics for porous burners, have in their composition alumina and silicon carbide which is the material of the porous inserts of this work. These materials provide high temperature resistance, chemical stability and low thermal degradation, a factor that increases longevity over traditional burners. In addition, these materials have relatively low cost (Gao, et al., 2014a).

Porous media is characterized by volumetric porosity and linear pore density. The smaller the pore size, the greater the difficulty of flame propagation, which justifies the burner of this work to have 2 different regions. This is because, when pore size is decreased, the area increases (m^2 / m^3) between the gas and solid phases. This increase in the area of heat exchange between the phases allows a greater transfer of energy from the gases to the porous matrix, decreasing the flame temperature and making it more difficult to propagate (Trimis and Durst, 1996). It is used as a barrier for the flame front. A very common investigated design of the porous radiant burner consists of a monolith with two different regions: a preheating region (PR) made of porous medium with small pore size placed upstream and a stable burning region (SBR) (Francisco, et al., 2010). This concept of two regions is used in this work, but for different configurations.

The current study comparatively investigates the LPG/air premixed combustion in a porous burner for two different configurations. The first geometry designated as A has two diameters of porous media and the second geometry named as B with only one diameter of porous media. The most common geometry used for porous burners has the same diameter of porous medium as show in the work by Catapan (2005), Panigrahy, et al., 2016 and many others. A change of the geometry can result in a change of the operating conditions and the performance. Therefore, there is a need to study new possibilities for geometries of porous burner. It is a way to expand the possibilities of manufacturing. The objective of the present work is to compare the performance of a porous burner with two different configurations. One with constant

porous medium area and the other with smaller downstream area and bigger length. With configuration A the flame velocity has two values: it's greater in the downstream region.

2. EXPERIMENTAL SECTION

2.1 Porous Burner

The porous burner apparatus is shown in Fig.1 and its dimensions in Fig. 2 for the two configurations. The burner is a stainless-steel tube of 120 mm diameter. The porous foams are made of silicon carbide with 80% volumetric porosity with 40 ppi for the preheating region and 10 ppi for the stable burning region (Fig. 2). The burner with geometry A is made with 5 porous inserts. The first two near the base are 70 mm in diameter and 20 mm in thickness. In sequence, the other 3 are 50 mm in diameter and 20 mm in thickness. For the other geometry B, there were 4 porous medium with the same diameter of 70 mm. The porous inserts are made of silicon carbide. The one lower porous medium constitutes the preheating region (PR) and the others the stable burning region (SBR).

The porous medium was insulated by a 20 mm thick Kaowool high temperature insulation material, for temperatures up to 1400°C. The injection plate is a high temperature Kaowool thermalboard with a thickness of 51 mm, for temperatures up to 1600°C. The reactants are injected by 5 tubes positioned in the base of the burner. Furthermore, were made 1 mm holes in the thermalboard.

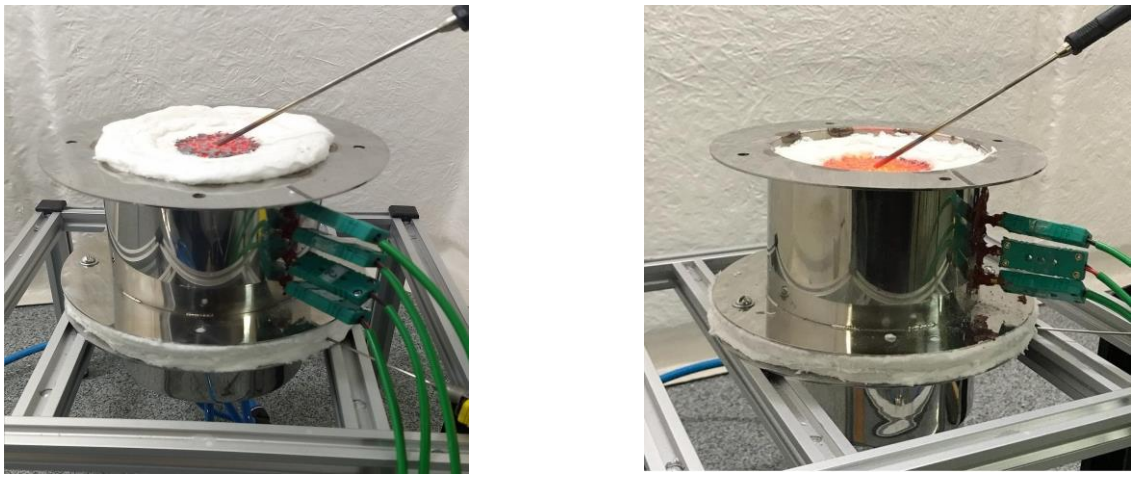

(a) Geometry A (b) Geometry B

Figure 1. Photograph of the porous burner.

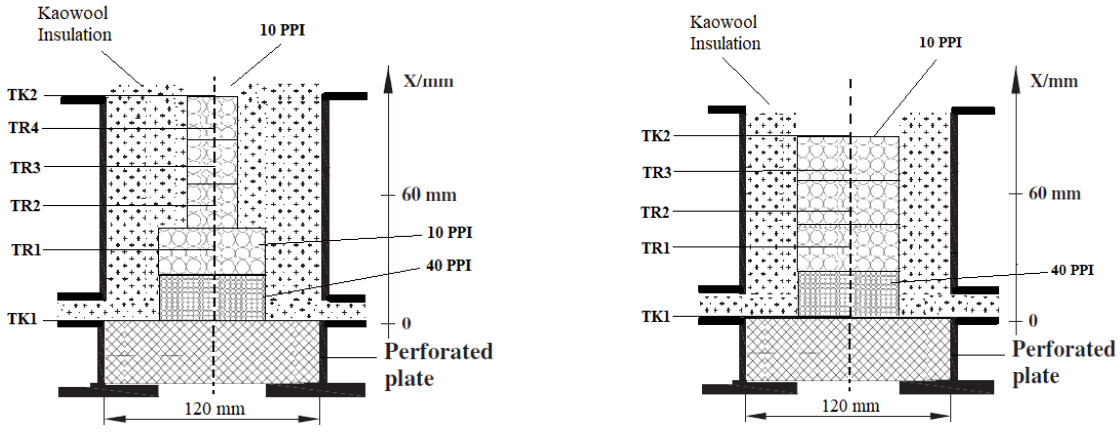

(a) Geometry A (b) Geometry B

Figure 2. Dimensions of the porous burner for two different geometries.

Thermocouples type K and R were used in the experiment, as shown Fig. 2. The thermocouple type K was positioned on the porous burner surface and between the insulation plate and the first porous medium. In addition, the temperature of the insulation plate was limited at 1000°C to avoid damage and flame flashback.

2.2 Experimental Setup and Techniques

Figure 3 shows the burner arrangement with all components of the experiment, which includes a burner, a fuel/air supply system and a data measurement system. The fuel supply system consists of a control valve, a locking valve and a pressure valve connected to a GLP cylinder. The air supply system has a control valve and treatment filters. For each line, there are a flow controller and flow meter specific to each gas. Laboratory air was supplied using a compressor connected to an air storage tank. Table 1 shows a list of the main equipments of this work.

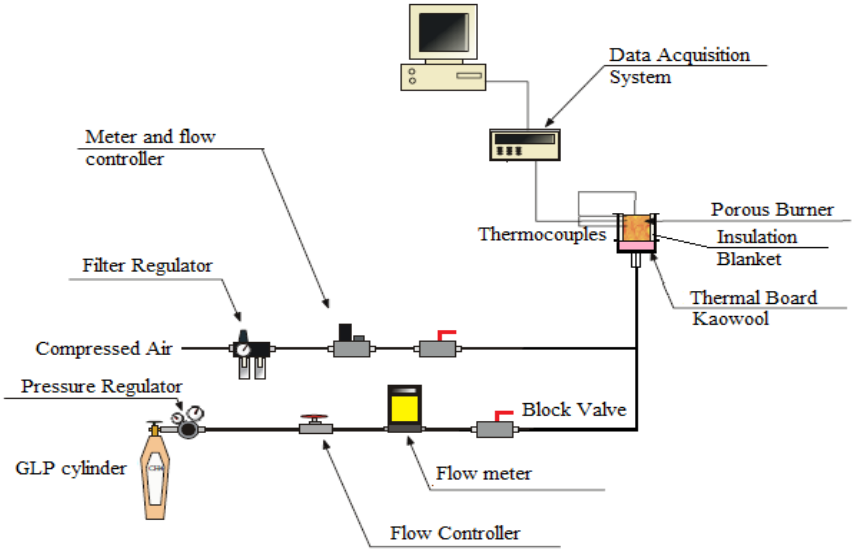

Figure 3. Schematic of the experimental system. Adapted from Pereira, 2002.

Table 1. List of the main equipments used in this work.

Equipment	Brand	Model
Air Flow Meter	Alicat	M-100SLPM-D/5M
Fuel Flow meter	Omega	FMA-A2307
Data Acquisition System	Novus	Fieldlogger

For data acquisition, was used a system with 8 analog channels for temperature measurement. The equipment for data acquisition has a software that is possible to control the temperatures in real time and after that collect the data. To solve all the equations and obtain the parameters for the experiments, the software Engineering Equation Solver was used.

In this study, LPG was the fuel supply for the experiments with the porous burner. All the results are based in the combustion of the premixed reagents. With GLP being a mixture, the properties of the gases were approximated as propane gas (Huzayyin, et al., 2008). The fuel gas flow meter measurement scale was limited to 3 liters per minute. Due to these restrictions, the operation diagram and the parameters analyzed in this work were also limited, as shown in the results section.

Initially, an equivalence ratio of Φ=0.8 is set and the flame is ignited at the burner top. After a few minutes, the flame front penetrates the porous medium indicated by a rise in the thermocouples. The heating process takes about 15 minutes and then the desired test condition is set. After that, when the temperatures remain constant for at least 20 minutes, the results are collected for each condition. This procedure is similar for the two configurations of this study.

The flame stability limits were determined by keeping the equivalence ratio constant and varying the thermal power of the burner. The lower stability limit (LSL) was obtained when the temperature of the thermocouple TK1 reaches 1000ºC. The upper stability limit (USL) was obtained when the flame detachment occurs and the blue flame is observed on the burner outlet surface or due to the flow limit of the flow meter. The equivalence ratio set in this study was Φ = 0.47. With this value, the temperatures along the burner did not exceed the temperature supported by the porous media (1400ºC).

Below are listed some of the main parameters and equations used in this work (Catapan, 2005). The radiation efficiency is defined as:

$$\eta_{rad} = \frac{\dot{Q}_{rad}}{Sr} . \tag{2.1}$$

$\dot{Q}_{rad}$ is the radiation heat flux on the surface of the burner, here defined as:

$$\dot{Q}_{rad} = \varepsilon * \sigma * \left({T_{sup}}^4 - {T_{amb}}^4\right) * A_q , \tag{2.2}$$

with ε the burner emissivity, σ the Stefan-Boltzmann constant and A_q the burner surface area.

As a reasonable approximation, the radiation temperature was the one measured by thermocouple TK2 and the radiation emissivity on the porous burner surface was assumed as equal to 1.0, since this porous media has high optical penetration (Catapan, 2005).

S_r is the burner thermal power and is given by Eq. (2.3):

$$S_r = \dot{m}_c \Delta h_{r,c}, \tag{2.3}$$

where $\dot{m}_c$ is the mass flow rate of the fuel and $\Delta h_{r,c}$ is the low calorific power.

According to Beckwith, et al., 2007, for a quantity defined as a function of others through a functional relation of the type $y = f$ (x_1, x_2, ..., x_n), the resulting measurement uncertainty is given by:

$$IM_y = \sqrt{\left(IM_{x1} * \frac{\partial y}{\partial x_1}\right)^2 + \left(IM_{x_n} * \frac{\partial y}{\partial x_n}\right)^2}, \tag{2.4}$$

where IM_y is the total measurement uncertainty for y function. IM_{x_n} represents the uncertainty of each measurement system. Finally, x_n represents the variable measured for each measurement system.

The total uncertainty associated calculated with Eq. (2.4) for the burner equivalence ratio, thermal power and radiation efficiency were estimated in Table 2. Maximum uncertainty for equivalence ratio and power are acceptable, but radiation efficiency shows a discrepancy. It is related to dependence of more uncertainty parameters as showed in Eq. (2.1).

Table 2. Measurement Uncertainty for the burner equivalence ratio, thermal power and radiation efficiency.

Measurement Uncertainty				
Configuration	**A**		**B**	
	maximum	**minimum**	**maximum**	**minimum**
Φ	0.08	0.016	0.04	0.017
Power (kW)	0.04606		0.04606	
Radiation efficiency (%)	2.09	0.29	1.28	0.51

3. RESULTS AND DISCUSSION

The results demonstrate that the designed burner works within acceptable parameters. The burner was operated only with ϕ = 0.47 for configurations A and B.

The operation diagram is one of the most important parameters of the porous burner. This represents the range stability that the flame can be sustained in the porous burner, without any problem to the components, flame flashback or flame detachment. Table 3 shows the operation points and stability limits obtained in the present work for both configurations.

Table 3. Operation points obtained from tests.

	Power(kW)	
Configuration	**A**	**B**
Lower stability limit	0.3	0.63
Operating range	0.7	0.75
	0.9	0.88
	1.1	1.13
	1.4	1.38
Upper stability limit	1.6	1.51

The operating points shows the upper and lower stability limits. In order to obtain this diagram operation for equivalence ratio equal to 0.47, it was necessary to vary the thermal power keeping the same equivalence ratio, monitoring the temperatures of the insulated plate and the surface of the burner (thermocouples TK1 and TK2). The burner with the configuration A presented the largest operating range due to the longer burner length, that is, a larger number of ceramic pieces (see Fig. 2).

Figure 4 shows the effect of the geometry on the temperature distributions along the centerline as a function of the axial position, for various burner thermal power. The temperature measured by thermocouples TK1, TR1, TR2 and TR3 are approximately in the same axial position for both configurations. The temperature profile for configuration B has only 5 points because of its length as shown in Fig. 2.

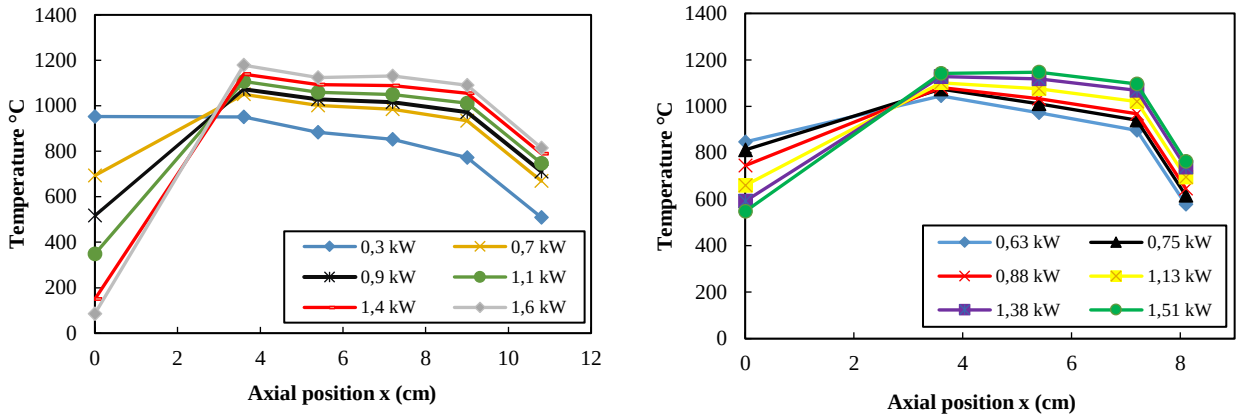

(a) (b)

Figure 4. Temperature distribution as a function of the axial position, for (a) configuration A and (b) configuration B.

The increase of the thermal power moves the flame front to the burner outlet surface. Also, the reaction zone temperature increases with the increase of the thermal power. These behaviors are agree with the studies of Francisco, et al., 2010 and Gao et al., 2014b. For all test conditions, the maximum reaction temperature obtained was 1180°C. With the temperature profile is possible to estimate the flame front region, since it is where the temperature reaches the highest values. Also, the results showed a sudden increase of the temperature gradient in the interface of the two layers of porous medium for both geometries. It indicates a drastic heat release from the post combustion region. As mentioned by Al-attab, et al., 2015, this proves the excess enthalpy theory that the high temperature porous medium layer serves as a media of quick solid–gas heat recirculation.

Figure 5 shows a comparison between the temperature distribution along the burner length for both geometries (A and B), with the approximately same thermal power (Sr = 0.9 kW).

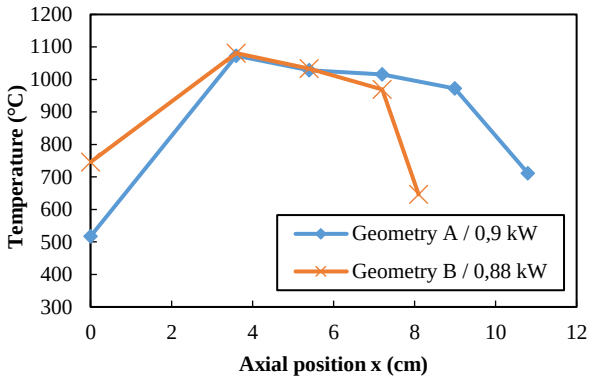

Figure 5. Flame front temperature along the burner length for geometry A and B.

For both configurations, the flame front was located near to the TR1 thermocouple region. The decrease of area in configuration A has not expressive changes in this region, since it is located at x = 4 cm. It is notable that the temperature profile has not big changes, only in the output region where configuration A has a bigger length. Also, the temperature difference between the two surfaces is about 9% for 0,9kW.

According to Gao, et al., 2014a, the flame temperature is dependent on the heat released via combustion, heat loss, and heat transferred from the combustion to the upstream and the downstream in the burner. In this study, the thermal radiation loss transferred downstream in the burner was an approximation and Fig. 6 shows the radiation efficiency of the present burner as a function of the power for two configurations. As can be seen, the radiation efficiency decreases with power or flame velocity. This behavior is agree with the literature and the work of Francisco, et al., 2010, Li and Hsu (2006). As expected, the burner with geometry B showed better radiation performance even with higher temperatures of the burner with geometry A (Fig. 7). This is because of the output area of the burner. Geometry A has less surface area than the other configuration.

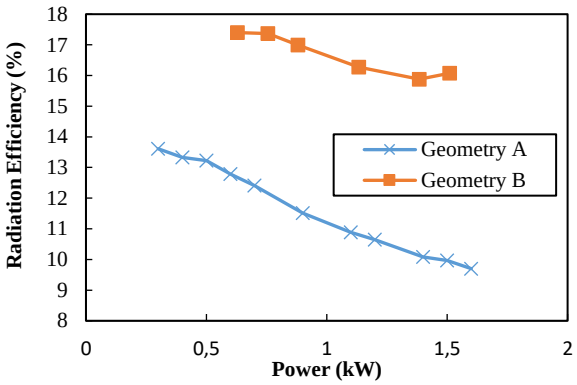

Figure 6. Radiation efficiency as a function of power for the two geometries.

As the flame velocity increases for a certain equivalence ratio, higher is the surface temperature. It may be caused by the move of the flame front upwards the burner surface and consequently an increase in the heat exchange with the ambient. Figure. 7 shows this behavior.

Also, for the same thermal power, the radiation efficiency of the configuration B was higher than configuration A, even though the surface temperature was lower (Fig.7). This effect occurred because the output surface area of the burner B is almost 50 % higher than configuration A.

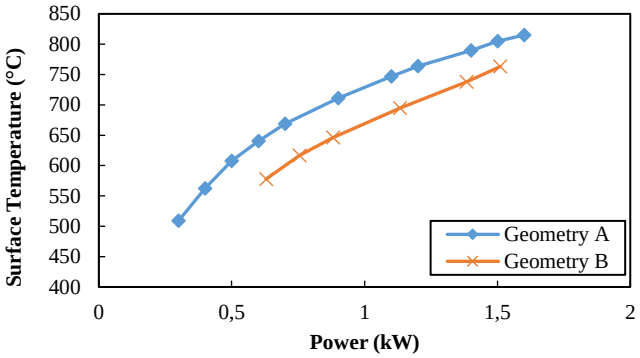

Figure 7. Surface temperature as function of power for the two geometries.

The increase of the thermal power moves the flame front to the burner outlet surface, increasing the surface temperature (Fig. 7). This effect was observed for both configurations tested. The maximum surface temperature obtained was 850 ºC, for configuration A with Sr=1.5 kW and Φ = 0.47.

For Sr=1.0 kW, the configuration A showed a surface temperature 9% higher than Configuration B. This effect was a result of the lower porous medium volume of the Configuration A, around of 11% less (considering just the porous volume).

4. CONCLUSIONS

In the present work two different geometries of the porous burner was built and tested using premixed air and fuel (LPG). The results obtained for the profile temperature, operating parameters and the radiation efficiency are consistent with the literature. The temperatures profile showed that the location of the flame front was almost the same for both configurations and the results showed that the burners had the same behavior for both geometries. However, the Configuration A showed a larger operation range due to its higher length.

Also, for the same thermal power, the configuration B resulted a radiation efficiency 5,3% higher because of the larger surface area of the burner.

The next step is to repeat the experiment using methane/air premixed and obtain the temperature profile on porous burner for a wide range of equivalence ratio and thermal power. Following, the CO emissions will be evaluated for both situations and compared.

5. REFERENCES

Al-attab, K. A., Ho, J. C., & Zainal, Z. A. 2015. "Experimental investigation of submerged flame in packed bed porous media burner fueled by low heating value producer gas". *Experimental Thermal and Fluid Science*, *62*, 1–8. <https://doi.org/10.1016/j.expthermflusci.2014.11.007>

Beckwith, Thomas G., Marangoni, Roy D., Lienhard John H. 2007. *Mechanical Measurements*. Pearson Prentice Hall. 6th edition.

Catapan, R. C., 2005. “Desenvolvimento Experimental de Queimadores Porosos Radiantes a Gás Natural”. *Monography*. Federal University of Santa Catarina. Florianópolis, Brazil.

Francisco, R. W., Rua, F., Costa, M., Catapan, R. C., & Oliveira, A. A. M. (2010). "On the combustion of hydrogen-rich gaseous fuels with low calorific value in a porous burner". *Energy and Fuels*, *24*(2), 880–887. <https://doi.org/10.1021/ef9010324>

Gao, H. B., Qu, Z. G., Feng, X. B., & Tao, W. Q. 2014a. "Methane/air premixed combustion in a two-layer porous burner with different foam materials". *Fuel*, *115*, 154–161. <https://doi.org/10.1016/j.fuel.2013.06.023>

Gao, H., Qu, Z., Feng, X., & Tao, W. 2014b. "Combustion of methane/air mixtures in a two-layer porous burner: A comparison of alumina foams, beads, and honeycombs". Experimental Thermal and Fluid Science, 52, 215–220. <https://doi.org/10.1016/j.expthermflusci.2013.09.013>

Hsu, P. (2006). "Emissions and radiation efficiency for methane combustion within a porous ceramic burner". Clean air, 7, 285–302. <https://doi.org/10.1615/InterJEnerCleanEnv.v7.i3.70>

Huzayyin, A. S., Moneib, H. A., Shehatta, M. S., & Attia, A. M. A. (2008). "Laminar burning velocity and explosion index of LPG-air and propane-air mixtures". Fuel, 87(1), 39–57. <https://doi.org/10.1016/j.fuel.2007.04.001>

Panigrahy, S., Mishra, N. K., Mishra, S. C., & Muthukumar, P. 2016. "Numerical and experimental analyses of LPG (liquefied petroleum gas) combustion in a domestic cooking stove with a porous radiant burner". *Energy*, *95*, 404–414. <https://doi.org/10.1016/j.energy.2015.12.015>

Pereira, F. M., 2002. “Medição de características térmicas e estudo do mecanismo de estabilização de chama em queimadores porosos radiantes”. *Dissertation*. Mechanical Engineering Department, Federal University of Saint Catherine. Florianópolis, Brazil.

Wood, S., & Harris, A. T. 2008. "Porous burners for lean-burn applications". *Progress in Energy and Combustion Science*, *34*(5), 667–684. <https://doi.org/10.1016/j.pecs.2008.04.003>

6. RESPONSIBILITY NOTICE

The authors are the only responsible for the printed material included in this paper.